




Effect of the Incorporation of Bactericidal Agents Ag, Cu, and Zn Through Micro-arc Oxidation on the Properties of the Ti-25Ta Alloy Surface

Pedro Akira Bazaglia Kuroda^{a,b*} , Giovana Collombaro Cardoso^c, Mariana Correa Rossi^a,
Carlos Roberto Grandini^c , Conrado Ramos Moreira Afonso^a 

^aUniversidade Federal de São Carlos (UFSCar), Materials Engineering Department (DEMa),
13565-905, São Carlos, SP, Brasil.

^bUniversidade Federal da Integração Latino-Americana (UNILA), Instituto Latino-Americano de
Ciências da Vida e da Natureza (ILACVN), 85870-650, Foz do Iguaçu, PR, Brasil.

^cUniversidade Estadual Paulista (UNESP), Laboratório de Anelasticidade e Biomateriais,
17033-360, Bauru, SP, Brasil.

Received: September 19, 2023; Revised: January 11, 2024; Accepted: April 03, 2024

The main objective of this paper is to produce an anodic layer of TiO₂ rich in calcium, phosphorus, and magnesium using the anodizing technique known as micro-arc oxidation (MAO) on the Ti-25Ta alloy together with the incorporation of silver (Ag), copper (Cu) and zinc (Zn) metallic ions using different electrolytes. The structural changes and microstructures on the MAO surfaces were analyzed using the X-ray diffraction (XRD) technique and scanning electron microscopy (SEM). The chemical composition to verify whether silver, copper, and zinc were incorporated via energy dispersive spectroscopy (EDS) and surface characteristics such as wettability and hardness of the coatings were also investigated. From the EDS mapping results, it is observed that the MAO process was effective in incorporating the ions present in the electrolyte. Regarding X-ray diffraction patterns, the TiO₂ phases formed in the Ti-25Ta alloy has a mixture of anatase and rutile, making the MAO surface hydrophilic. The Ag element surface is thicker than the films containing Cu and Zn, as the Ag ions have high electrical conductivity, accelerating the oxidation process during surface treatment. Regarding hardness, coating containing Cu have a higher hardness value.

Keywords: Bactericidal agents, surface modification, Ti alloy, ion incorporation, biomaterial.

1. Introduction

Commercially pure titanium (CP-Ti) and its alloys have excellent properties, including biocompatibility, good corrosion resistance, high specific strength, and low density, making them interesting for use in materials for implants and medical devices^{1,2}. Tantalum (Ta), as niobium (Nb) and molybdenum (Mo), are β -stabilizing element that reduces the transition temperature from the α phase (hexagonal closest-packed (hcp) crystalline structure) to the β phase (body-centered cubic (bcc) crystalline structure) of the Ti³. For applications in orthopedic implants, it is interesting to use these alloy elements since the β phase of Ti has better mechanical properties than the α phase, which can reduce stress shielding effects^{4,5}.

Thus, the Ti-Ta alloy system was extensively studied for potential use in the biomedical field⁶⁻¹¹. Zhou et al.^{8,9} studied the Ti-Ta system and observed that its alloys exhibited better cytotoxicity results than the Ti-6Al-4V ELI alloy. The addition of Ta improved the corrosion resistance of Ti due to the formation of a more resistant Ta₂O₅ passivation film than TiO₂. Moreover, alloys between 20 and 30 wt% of Ta had better elastic modulus results. In a more detailed study of the quenched Ti-25Ta alloy, Zhou et al.¹⁰ found that the

presence of the α -orthorhombic phase, with a larger unit cell volume, gave the lowest elastic modulus for this alloy among the studied alloys of the system.

Although the good properties of Ti alloys are attractive for their use as biomaterials for orthopedics implants, their surface still exhibit relatively low biological activity and resistance to corrosion and wear¹². Thus, surface modification techniques such as plasma spray^{13,14}, sol-gel^{15,16}, and micro-arc oxidation (MAO)^{17,18} have been studied to improve the surface properties of Ti and its alloys.

In addition, problems associated with infection of the implants are also very frequent, making it interesting to obtain a mechanism of bacterial action on the surface of the alloys, which can prevent the formation of biofilms after the surgical procedure¹⁹. Therefore, antibacterial agents can be incorporated into the surface through the MAO method to reduce bacterial adhesion and proliferation on the material's surface. For this purpose, zinc (Zn)^{20,21}, silver (Ag)^{22,23}, and copper (Cu)^{24,25} are examples of elements that can be used during MAO treatment to attribute antimicrobial properties to Ti and its alloys^{26,27}.

The bactericidal action mechanisms of these elements have some differences between them. Zn or ZnO nanoparticles generate reactive oxygen species (ROS), which kill bacteria.

*e-mail: pedro.kuroda@ufscar.br

Ag particles infiltrate the bacteria's nucleus, damaging their DNA. Finally, bacteria contact with Cu ions generates cavities in the cell wall¹⁹.

The surface modification of the Ti-25Ta alloy through MAO treatment was studied by Kuroda et al.²⁸. They found that the oxide layer formed on the surface of the alloy by this method improved the material's wear resistance. Furthermore, it was observed that in the MAO coating produced on Ti-25Ta, titanium dioxide (TiO₂) forms in two crystalline structures, anatase and rutile. According to other works in the literature, TiO₂ rich in rutile has more excellent resistance to wear due to its high hardness value compared to TiO₂ in the form of anatase^{29,30}. Thus, this study aimed to continue the investigations regarding the surface modification of the Ti-25Ta alloy, verifying the effect of adding different bactericidal agents (Ag, Cu, and Zn) on the characteristics and properties of the coating produced by the MAO technique. This study also sought to compare the effect of each bactericidal element produced on the MAO surface characteristics, which can also influence the material's response against infectious agents.

2. Material and Methods

A 60 g ingot of Ti-25Ta alloy was prepared using an arc melting furnace with a water-cooled copper crucible, a non-consumable tungsten electrode, and a controlled argon atmosphere. MAO treatments were performed in a DC power source (Keysight, N5751A) at 300 V, 2.5 A, at room temperature, for 60 s. The electrolyte used consisted of 0.35 M calcium acetate monohydrate ((CH₃COO)₂Ca · H₂O), 0.02 M β-glycerol phosphate pentahydrate (C₃H₇Na₂O₆P · 5H₂O), and 0.1 M magnesium acetate tetrahydrate ((CH₃COO)₂Mg · 4H₂O) to incorporate Ca, P, and Mg³¹. To incorporate Ag, Cu, and Zn, were used 2.5 mMol silver nitrate (AgNO₃), 2.5 mMol copper chloride (CuCl₂), and 1.0 mMol zinc chloride (ZnCl₂). The concentration of each bactericidal element was determined after a literature analysis^{21,22,32}.

The MAO coatings were characterized by x-ray diffraction using a MiniFlex600 diffractometer (Rigaku, Tokyo, Japan) with Cu Kα radiation (λ = 1.54056 Å). Optical microscope (Olympus BX51M), scanning electron microscopy, SEM (Carl Zeiss Inc), and confocal laser scanning microscopy, CLSM (Leica, DC3M) were used to analyze microstructure, topographic images, roughness by CLSM, and cross sections of MAO coating. Wettability was obtained using contact angle measurements by the droplet technique on a Krüss DSHAT HTM Reetz GmbH. Deionized water, 2.5 μl volume, was used as the test fluid.

To obtain the Vickers microhardness values, a Shimadzu HMV G20ST was used by applying 0.5 kgf for 15 s following ASTM-E384³³ through an average of 15 measurements. In order to analyze the adhesion of the MAO films to the Ti-25Ta substrates, the Rockwell-C adhesion test was performed³⁴. This test was carried out using a Sussen Wolpert brand Rockwell C indenter with a load of 150 kg.

3. Results and Discussions

Figure 1 shows the variation in current during the MAO layer formation on the Ti-25Ta alloy with incorporation of Ca,

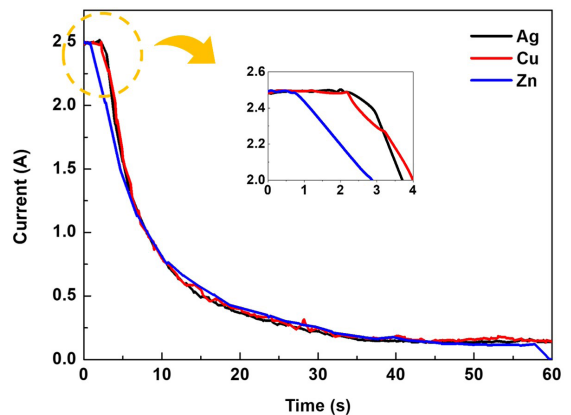


Figure 1. Current x time curves of the Ti-25Ta alloy during the MAO layer formation with incorporation of Ca, P and Mg as well as Ag, Cu and Zn elements.

P and Mg as well as Ag, Cu and Zn, considering bactericidal elements. The MAO process carried out in this work initially operates in the galvanostatic regime (constant current value). As the MAO coating grows during the surface modification process, the voltage value increases until reaching its limit value (300 V). After reaching 300V, the current value begins to decrease, and the process start to operate in the potentiostatic regime. More details of the surface modification process used in this work can be seen in previous works²⁹.

From Figure 1 also it can be seen the incorporation of Ag and Cu present a similar curve of current (A) x time (s), with dwell time in the galvanostatic regime of approximately two seconds. For the Zn incorporation process, the galvanostatic regime lasted just one second. This difference is due to the change in the electrical conductivity of the electrolyte, as the elements Ag and Cu have similar electrical conductivity values (62.5 and 61.7 Sm/mm²) the material can remain in the galvanostatic regime for longer. However, for the incorporation of Zn which has an electrical conductivity of 17.8 Sm/mm², the system reaches the limit voltage value (300V) to produce the MAO film.

The x-ray diffraction results performed on the surfaces of the Ti-25Ta alloy after the MAO process for incorporating the elements Ca, P, and Mg, with elements considered bactericidal, such as Ag, Cu, and Zn, are shown in Figure 2. Information about the XRD results of the substrate can be found in a previous study³⁰. The diffractograms showed characteristic peaks of the hexagonal closest-packed structure (HCP), known as the α phase in titanium alloys³⁵. In addition, characteristic peaks of titanium dioxide (TiO₂) in anatase and rutile forms can be visualized³⁶, indicating that the MAO process oxidized the Ti present in the Ti-25Ta alloy substrate. The diffraction peaks of the brookite structure on TiO₂ were not observed.

The anatase and rutile ratio (A/R) remains constant at approximately 2.3 in all diffractograms, indicating that the addition of CuCl₂, ZnCl₂, and AgNO₃ compounds to the electrolyte does not affect the formation of TiO₂ phases in the MAO coating.

No crystalline structures of compounds that can form easily during the MAO process, such as calcium and magnesium carbonates (CaCO₃ and MgCO₃), were observed due to the low concentrations of elements present in the electrolytes,

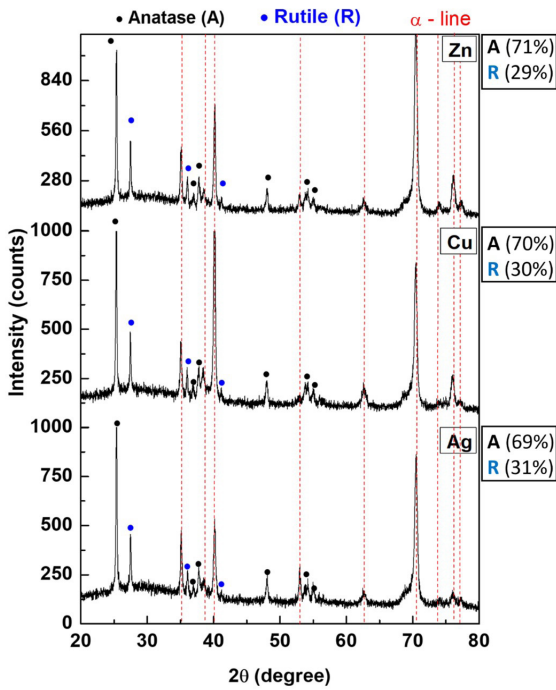


Figure 2. XRD of the MAO coatings containing Ag, Cu, or Zn on the Ti-25Ta substrate.

specifically Ag, Cu, and Zn, which can have cytotoxic character in high amounts^{37,38}.

Figure 3 shows the SEM images at 1000x and 10,000x magnifications on the MAO surface of the Ti-25Ta alloy. Kuroda et al.³⁰ presented the SEM image of the Ti-25Ta substrate, without the MAO coating. It was observed that the MAO process produced a porous surface typical of the MAO coatings. The pores come from oxygen bubbles forming in the electrolyte during the formation of electric arcs, which can reach temperatures above 2000 °C^{39,40}. Generally, the more intense the electric arcs produced during the MAO process, the larger the oxygen bubbles from boiling water, forming anodic films with high porosity.

From the SEM topographic images, histograms were produced (Figure 4) to demonstrate the size and quantity of pores visualized on the surfaces of the Ti-25Ta alloy containing Ag (Figure 4a), Cu (Figure 4b) and Zn (Figure 4c). The histograms showed that most pores present in the MAO layer have an average area of 0.25-0.50 μm². Figure 4d shows the relationship between the number of pores per μm², considering the error bar it can be highlighted that the surfaces of the alloys have the same number of pores per unit area.

Kuroda et al.³⁰ produced a MAO layer rich in Ca, P and Mg in the Ti-25Ta-Zr system alloys (Zr = 0, 25 and 50% by weight), and was observed that the majority of ceramic pores produced on the alloy surfaces have a size

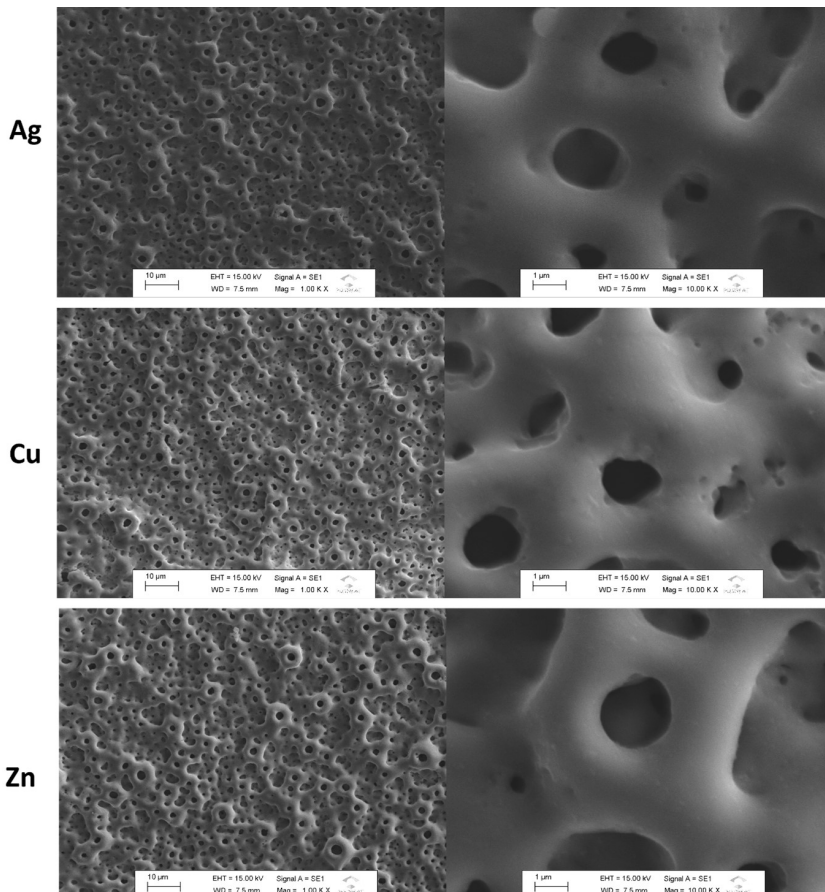


Figure 3. SEM images at 1000x (left) and 10000x (right) of the MAO coatings containing Ag, Cu, or Zn on the Ti-25Ta substrate.

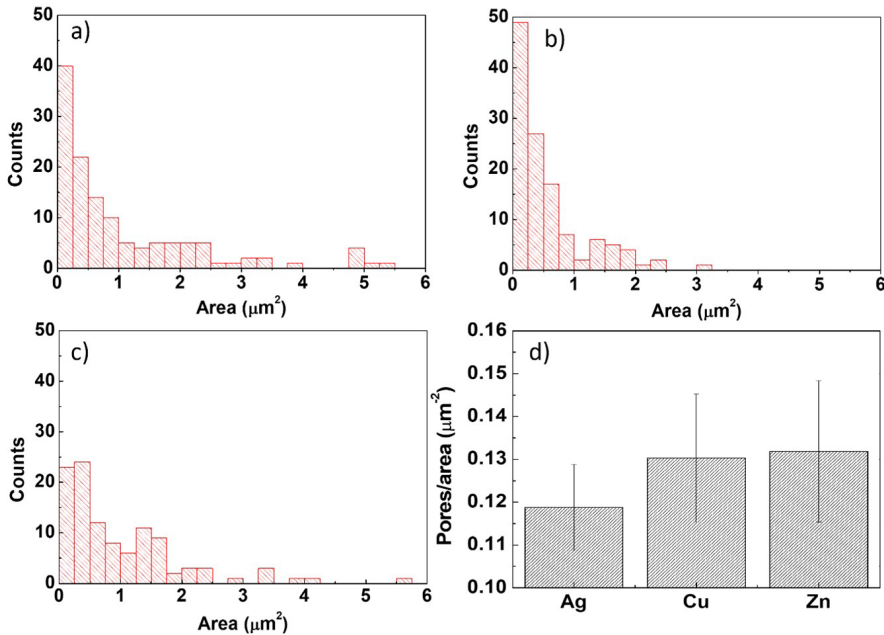


Figure 4. Histograms produced from SEM images of the ceramic layer formed on the Ti-25Ta alloy. a), b) and c) number of pores per area. d) relation of pores/area from each surface modified with Ag, Cu and Zn ions.

of approximately $0.50 \mu\text{m}^2$, and α -type alloys tend to have larger pores compared to β -type alloys. It is observed that the results obtained by Kuroda corroborate the results obtained in this work. Figure 5 shows the cross-section images of the MAO coating with the incorporation of Ag, Cu, or Zn ions and the chemical mapping images of the elements present in the substrate (Ti and Ta) on the MAO coating.

It was observed that the MAO process effectively incorporated the chemical elements in the electrolytes, noting that Ca, P, and Mg, along with Ag, Cu, or Zn, are present in all coatings. Furthermore, the coatings exhibit a significant level of carbon content. This carbon originates from the Ca, Mg, and P acetates, which may hinder the formation of electric arcs due to its property of reducing the electrolyte's electrical conductivity. However, based on the EDS results, it is observed that the MAO process successfully incorporated the metallic ions. To complement the semi-quantitative chemical composition results, Figure 6 shows the chemical composition of Ca, P, Mg, Ag, Cu, and Zn in the MAO coatings produced on the Ti-25Ta alloy.

Previous studies in the literature have shown that in MAO coatings, which were produced in a similar way as described in this, Zn, Cu, and Ag are commonly found in the form of $\text{ZnO}^{20,41}$, Cu_2O and $\text{CuO}^{24,41}$, and Ag_2O and metallic Ag⁴², respectively.

Regarding the cross-section images, it was observed that the coating containing Ag has a thickness of $(31.8 \pm 2.5) \mu\text{m}$. The surface containing Cu has a thickness of $(9.1 \pm 1.2) \mu\text{m}$, while the MAO surface containing Zn has a thickness of $(9.9 \pm 1.0) \mu\text{m}$. The MAO coatings with Cu and Zn are thinner because chlorides (ZnCl_2 and CuCl_2) were used instead of the nitrate (AgNO_3).

Figure 7 is indicating the wettability results of the MAO surface and the 2D images of the contact of distilled water with the MAO coating on the Ti-25Ta alloy. Kuroda et al.³⁰

presented that the contact angle value of the Ti-25Ta alloy, without the MAO coating, is approximately 45° . The contact angle in all samples of this present study was less than 90° , indicating that the MAO surfaces produced in this study are hydrophilic. Previous studies reported that TiO_2 in the anatase form is generally hydrophilic, while TiO_2 in the rutile form creates hydrophobic surfaces. However, a mixture of these two phases generally results in hydrophilic surfaces⁴³. Based on XRD results, the MAO coatings on the Ti-25Ta substrate have an anatase/rutile ratio of approximately 2.3 and hydrophilic behavior as predicted by the literature, which contributes to increasing its bioactivity, improving its osseointegration⁴⁴.

Figure 8 presents the results of the surfaces' hardness by the Vickers microhardness technique. The coatings contain Ag, Cu, and Zn exhibit hardness levels of 337, 404, and 286 HV, respectively. According to Kuroda et al.⁴⁵, the Ti-25Ta alloy, after a solution heat treatment, has a hardness of approximately 250 HV. Therefore, it is observed that the coatings have higher hardness than the substrate, even with the high amounts of pores, which tend to decrease the hardness value of the MAO surfaces.

The surface with Cu has a higher hardness value than the MAO surfaces containing Ag and Zn. This behavior is due to the lower radius value and Cu's atomic weight than Ag and Zn. The element with a small atomic radius and low atomic weight is more easily incorporated into the MAO coating process. Therefore, the Cu-containing coating probably has a higher entropy, which results in a higher hardness. It is important to note that a hard anodic surface in Ti alloys is preferred to increase resistance to micro-abrasive wear. This is because surfaces with high hardness tend to have good wear resistance, as demonstrated by Kuroda et al.⁴⁶.

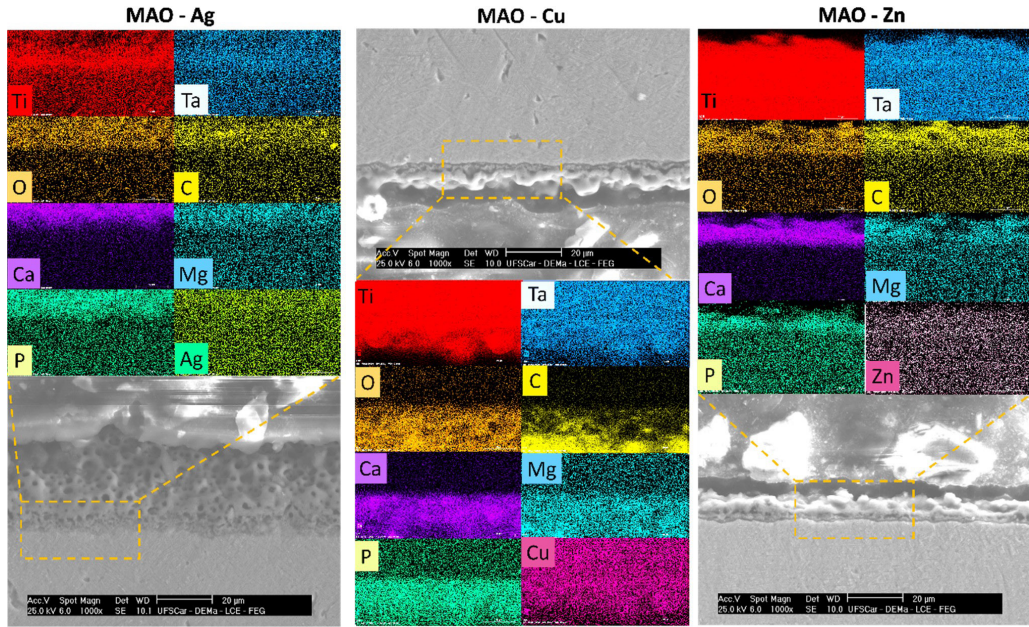


Figure 5. Chemical mapping by EDS of elements in the MAO coatings and cross-sectional images of the produced coatings on Ti-25Ta substrate.

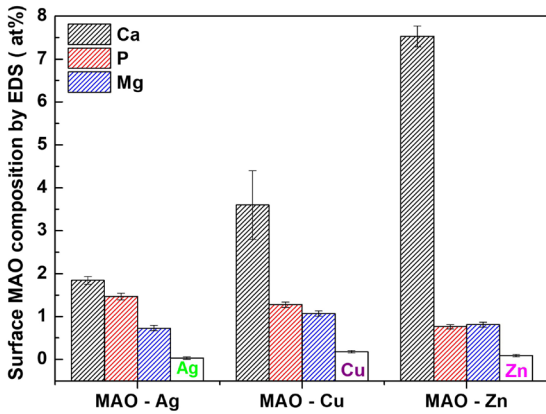


Figure 6. Elemental quantification obtained using EDS for Ti-25Ta alloys.

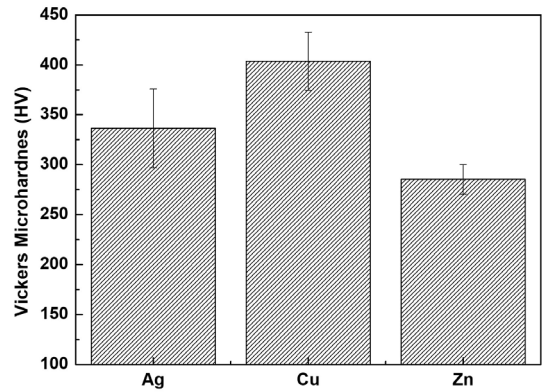


Figure 8. Vickers microhardness of the MAO coatings containing Ag, Cu, or Zn on the Ti-25Ta substrate.

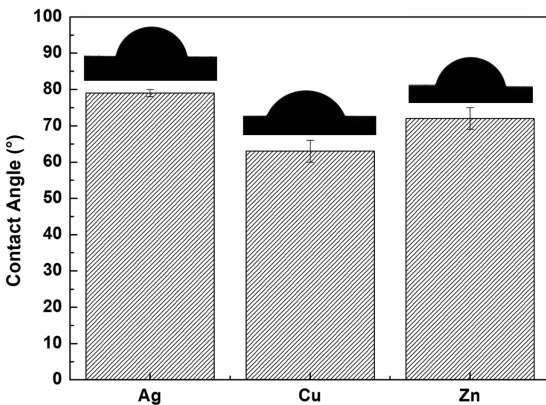


Figure 7. Contact angle of the MAO coatings containing Ag, Cu, or Zn on the Ti-25Ta substrate.

4. Conclusions

From the results obtained in this study, it can be concluded that:

- It was possible to incorporate bactericidal elements (Ag, Cu, and Zn) into the surface of the Ti-25Ta alloy using the MAO method.
- The Ag-containing coating has the highest thickness due to its superior electrical conductivity.
- The anatase/rutile ratio remained close to 2.3 in all coatings produced, indicating that adding Ag, Cu, or Zn to the electrolyte did not affect the formation of the TiO₂ phases.
- The proportion of anatase and rutile phases on the coatings ensured the surfaces were hydrophilic, with contact angles between 64-79°.

- The MAO surface containing Cu has higher hardness compared to the MAO surface containing Ag and Zn

5. Acknowledgments

The authors would like to thank the Faculdade de Ciências de Bauru, UNESP, for the XRD and SEM measurements. This study was supported by the following funding agencies FAPESP (São Paulo Research Foundation) grants #2019/26517-6 and through “Projeto Temático” # 2018/18293-8. This study was financed partly by the Coordenação de Aperfeiçoamento de Pessoal de Nível Superior of Brazil (CAPES), Finance Code 001”, and CNPq (Brazilian National Research Council), grant # 314.810/2021-8.

6. References

- Chen L-Y, Cui Y-W, Zhang L-C. Recent development in beta titanium alloys for biomedical applications. *Metals (Basel)*. 2020;10(9):1139.
- Li G, Ma F, Liu P, Qi S, Li W, Zhang K, et al. Review of micro-arc oxidation of titanium alloys: mechanism, properties and applications. *J Alloys Compd*. 2023;948:169773.
- Quadros FF, Kuroda PAB, Sousa KSJ, Donato TAG, Grandini CR. Preparation, structural and microstructural characterization of Ti-25Ta-10Zr alloy for biomedical applications. *J Mater Res Technol*. 2019;8(5):4108-14.
- Cardoso GC, Kuroda PAB, Grandini CR. Influence of Nb addition on the structure, microstructure, vickers microhardness, and Young’s modulus of new β Ti-xNb-5Mo alloys system. *J Mater Res Technol*. 2023;25:3061-70.
- Jung T-K, Semboshi S, Masahashi N, Hanada S. Mechanical properties and microstructures of β Ti-25Nb-11Sn ternary alloy for biomedical applications. *Mater Sci Eng C*. 2013;33(3):1629-35.
- Ikeda M, Komatsu S-y, Nakamura Y. The effect of ta content on phase constitution and aging behavior of Ti-Ta binary alloys. *Mater Trans*. 2002;43(12):2984-90.
- Wu CY, Xin YH, Wang XF, Lin JG. Effects of Ta content on the phase stability and elastic properties of β Ti-Ta alloys from first-principles calculations. *Solid State Sci*. 2010;12(12):2120-4.
- Zhou YL, Niinomi M, Akahori T. Effects of Ta content on Young’s modulus and tensile properties of binary Ti-Ta alloys for biomedical applications. *Mater Sci Eng A*. 2004;371(1):283-90.
- Zhou YL, Niinomi M, Akahori T, Fukui H, Toda H. Corrosion resistance and biocompatibility of Ti-Ta alloys for biomedical applications. *Mater Sci Eng A*. 2005;398(1):28-36.
- Zhou Y-L, Niinomi M. Ti-25Ta alloy with the best mechanical compatibility in Ti-Ta alloys for biomedical applications. *Mater Sci Eng C*. 2009;29(3):1061-5.
- Dobromyslov AV, Dolgikh GV, Dutkevich Y, Trenogina TL. Phase and structural transformations in Ti-Ta alloys. *Phys Met Metallogr*. 2009;107(5):502-10.
- Wang W, Zheng X, Yu F, Li Y, Xue X, Qi M, et al. Formation and cytocompatibility of a hierarchical porous coating on Ti-20Zr-10Nb-4Ta alloy by micro-arc oxidation. *Surf Coat Tech*. 2020;404:126471.
- Niu Z, Zhou W, Wang C, Cao Z, Yang Q, Fu X. Fretting wear mechanism of plasma-sprayed CuNiIn coating on Ti-6Al-4V substrate under plane/plane contact. *Surf Coat Tech*. 2021;408:126794.
- Gao Y, Shen K, Wang X. Microstructural evolution of low-pressure plasma-sprayed Ti-6Al-4V coatings after heat treatment. *Surf Coat Tech*. 2020;393:125792.
- Azzouz I, Khelifi K, Faure J, Dhiflaoui H, Larbi ABC, Benhayoune H. Mechanical behavior and corrosion resistance of sol-gel derived 45S5 bioactive glass coating on Ti6Al4V synthesized by electrophoretic deposition. *J Mech Behav Biomed Mater*. 2022;134:105352.
- Azari R, Rezaie HR, Khavandi A. Investigation of functionally graded HA-TiO₂ coating on Ti-6Al-4V substrate fabricated by sol-gel method. *Ceram Int*. 2019;45(14):17545-55.
- Cimenoglu H, Gunyuz M, Kose GT, Baydogan M, Ugurlu F, Sener C. Micro-arc oxidation of Ti6Al4V and Ti6Al7Nb alloys for biomedical applications. *Mater Charact*. 2011;62(3):304-11.
- Korkmaz K. The effect of Micro-arc oxidation treatment on the microstructure and properties of open cell Ti6Al4V alloy foams. *Surf Coat Tech*. 2015;272:72-8.
- Pesode PA, Barve SB. Recent advances on the antibacterial coating on titanium implant by micro-Arc oxidation process. *Mater Today Proc*. 2021;47:5652-62.
- Cardoso GC, Barbaro K, Kuroda PAB, Imperatori L, De Bonis A, Teghil R, et al. Incorporation of Ca, P, Mg, and Zn elements in Ti-30Nb-5Mo alloy by micro-arc oxidation for biomedical implant applications: surface characterization, cellular growth, and microorganisms’ activity. *Coatings*. 2023;13(9):1577.
- Shimabukuro M, Tsutsumi Y, Nozaki K, Chen P, Yamada R, Ashida M, et al. Chemical and biological roles of zinc in a porous titanium dioxide layer formed by micro-arc oxidation. *Coatings*. 2019;9(11):705.
- Zhang L, Li B, Zhang X, Wang D, Zhou L, Li H, et al. Biological and antibacterial properties of TiO₂ coatings containing Ca/P/Ag by one-step and two-step methods. *Biomed Microdevices*. 2020;22(2):24.
- Shimabukuro M, Tsutsumi Y, Yamada R, Ashida M, Chen P, Doi H, et al. Investigation of realizing both antibacterial property and osteogenic cell compatibility on titanium surface by simple electrochemical treatment. *ACS Biomater Sci Eng*. 2019;5(11):5623-30.
- Cardoso GC, Barbaro K, Kuroda PAB, De Bonis A, Teghil R, Krasnyuk II Jr, et al. Antimicrobial Cu-doped TiO₂ coatings on the β Ti-30Nb-5Mo alloy by micro-arc oxidation. *Materials (Basel)*. 2024;17(1):156.
- Shimabukuro M, Tsutsumi Y, Nozaki K, Chen P, Yamada R, Ashida M, et al. Investigation of antibacterial effect of copper introduced titanium surface by electrochemical treatment against facultative anaerobic bacteria. *Dent Mater J*. 2020;39(4):639-47.
- Shimabukuro M. Antibacterial property and biocompatibility of silver, copper, and zinc in titanium dioxide layers incorporated by one-step micro-arc oxidation: a review. *Antibiotics (Basel)*. 2020;9(10):716.
- He X, Zhang X, Wang X, Qin L. Review of antibacterial activity of titanium-based implants’ surfaces fabricated by micro-arc oxidation. *Coatings*. 2017;7(3):45.
- Kuroda PAB, de Mattos FN, Grandini CR, Afonso CRM. Micro-abrasive wear behavior by ball cratering on MAO coating of Ti-25Ta alloy. *J Mater Res Technol*. 2023;26:1850-5.
- Kuroda PAB, Rossi MC, Grandini CR, Afonso CRM. Assessment of applied voltage on the structure, pore size, hardness, elastic modulus, and adhesion of anodic coatings in Ca-, P-, and Mg-rich produced by MAO in Ti-25Ta-Zr alloys. *J Mater Res Technol*. 2023;26:4656-69.
- Kuroda PAB, dos Santos RFM, Rossi MC, Correa DRN, Grandini CR, Afonso CRM. Influence of Zr addition in β Ti-25Ta-xZr alloys on oxide formation by MAO-treatment. *Vacuum*. 2023;217:112541.
- Kuroda PAB, Grandini CR, Afonso CRM. Surface characterization of new beta Ti-25Ta-Zr-Nb alloys modified by micro-arc oxidation. *Materials (Basel)*. 2023;16(6):2352.
- Shimabukuro M, Hiji A, Manaka T, Nozaki K, Chen P, Ashida M, et al. Time-Transient effects of silver and copper in the porous titanium dioxide layer on antibacterial properties. *J Funct Biomater*. 2020;11(2):44.

33. ASTM International. E384–16, A.D., Standard Test Method for Microindentation Hardness of Materials. West Conshohocken: ASTM International; 2016.
34. Gemelli E, Scariot A, Camargo NHA. Thermal characterization of commercially pure titanium for dental applications. *Mater Res.* 2007;10(3):10.
35. Pesode P, Barve S. A review: metastable β titanium alloy for biomedical applications. *J Eng Appl Sci (Asian Res Publ Netw).* 2023;70(1):25.
36. Naji Chabuk QK, Salman Al-Murshdy JM, Dawood NM. Review: the surface modification of pure titanium by Micro-Arc Oxidation (MAO) process. *J Phys Conf Ser.* 2021;1973(1):012114.
37. Costa NA, Correa DRN, Lisboa-Filho PN, Sousa TSP, Grandini CR, Rocha LA. Influence of the molybdenum on characteristics of oxide films produced by micro-arc oxidation on Ti-15Zr-based alloys. *Surf Coat Tech.* 2021;408:126856.
38. Sousa TSP, Costa NA, Correa DRN, Rocha LA, Grandini CR. Morphology, crystalline structure and chemical composition of MAO treated Ti-15Zr-Mo surfaces enriched with bioactive ions. *Mater Res.* 2019;22(6):22.
39. Golubkov PE, Pecherskaya EA, Artamonov DV, Shepeleva JV. Method for measuring the micro-discharges temperature in the micro-arc oxidation process. *J Phys Conf Ser.* 2019;1393(1):012083.
40. Oliveira FG, Ribeiro AR, Perez G, Archanjo BS, Gouvea CP, Araújo JR, et al. Understanding growth mechanisms and tribocorrosion behaviour of porous TiO₂ anodic films containing calcium, phosphorous and magnesium. *Appl Surf Sci.* 2015;341:1-12.
41. Yang J, Fang K, Xu K, Shen X, Xu X. Effect of zinc or copper doping on corrosion resistance and anti-oxidative stress of strontium-based micro-arc oxidation coatings on titanium. *Appl Surf Sci.* 2023;626:157229.
42. Zhang L, Gao Q, Han Y. Zn and Ag Co-doped anti-microbial TiO₂ coatings on ti by micro-arc oxidation. *J Mater Sci Technol.* 2016;32(9):919-24.
43. Rossi MC, Santos RF, Kuroda PAB, Afonso CRM. Characteristics of ceramic-like coatings obtained by plasma electrolyte oxidation on different Ti alloys. *Bol Soc Esp Ceram Vidr.* 2023;63(1):33-46.
44. Zhang Z-Y, Huang T-Y, Zhai D-J, Wang H-B, Feng K-Q, Xiang L. Study on strontium doped bioactive coatings on titanium alloys surfaces by micro-arc oxidation. *Surf Coat Tech.* 2022;451:129045.
45. Kuroda PAB, Quadros FF, Afonso CRM, Grandini CR. The effect of solution heat treatment temperature on phase transformations, microstructure and properties of Ti-25Ta-xZr alloys used as a biomaterial. *J Mater Eng Perform.* 2020;29(4):2410-7.
46. Kuroda PAB, de Mattos FN, Grandini CR, Afonso CRM. Micro-abrasive wear behavior by ball cratering on MAO coating of Ti-25Ta alloy. *J Mater Res Technol.* 2023;26:1850-5.